Synthetic and Systems Biotechnology 10 (2025) 10–22

Contents lists available at ScienceDirect

Synthetic and Systems Biotechnology

journal homepage: www.keaipublishing.com/en/journals/synthetic-and-systems-biotechnology

Original Research Article

Biodegradation of combined pollutants of polyethylene terephthalate and phthalate esters by esterase-integrated *Pseudomonas* sp. JY-Q with surface-co-displayed PETase and MHETase

Haixia Wang, Jiahong Zhu, Meng Sun, Mengjie Gu, Xiya Xie, Tongtong Ying, Zeling Zhang, Weihong Zhong *

College of Biotechnology and Bioengineering, Zhejiang University of Technology, Hangzhou, 310032, Zhejiang Province, China

ARTICLE INFO

Keywords:
cOmpA
Cell surface co-display
PET
PAEs
Combined pollution
Pseudomonas sp. JY-Q

ABSTRACT

The waste pollution problem caused by polyethylene terephthalate (PET) plastics poses a huge threat to the environment and human health. As plasticizers, Phthalate esters (PAEs) are widely used in PET production and become combined pollutants with PET. Synthetic biology make it possible to construct engineered cells for microbial degradation of combined pollutants of PET and PAEs. PET hydroxylase (PETase) and mono-hydroxyethyl terephthalate hydroxylase (MHETase) isolated from *Ideonella sakaiensis* 201-F6 exhibit the capability to depolymerize PET. However, PET cannot enter cells, thus enzymatic degradation or cell surface displaying technology of PET hydrolase are the potential strategies. In this study, *Pseudomonas* sp. JY-Q was selected as a chassis strain, which exhibits robust stress tolerance. First, a truncated endogenous outer membrane protein cOmpA and its variant Signal (OprF)-cOmpA were selected as anchor motifs for exogenous protein to display on the cell surface. These anchor motifs were fused at the N-terminal of PET hydrolase and MHETase and transformed into *Pseudomonas* sp. JY-Q, the mutant strains successfully display the enzymes on cell surface, after verification by green fluorescent protein labeling and indirect immunofluorescence assay. The resultant strains also showed the catalytic activity of co-displaying PETase and MHETase for PET biodegradation. Then, the cell surface displaying PET degradation module was introduced to a JY-Q strain which genome was integrated with PAEs degrading enzymes and exhibited PAEs degradation ability. The resultant strain JY-Q-R1-R4-SFM-TPH have the ability of degradation PET and PAEs simultaneously. This study provided a promising strain resource for PET and PAEs pollution control.

1. Introduction

Polyethylene terephthalate (PET), a highly polymerized ester compound resulting from the combination of ethylene glycol (EG) and terephthalic acid (TPA) through ester bonds, is extensively utilized [1]. However, the significant accumulation of PET waste in the environment poses a serious threat to the ecosystem [2]. Traditional recycling methods for PET often involve chemical and mechanical approaches, utilizing hazardous reagents that can lead to secondary contamination and high energy consumption [3].

In 2016, a superbug known as *Ideonella sakaiensis* 201-F6 demonstrated the ability to completely break down low-crystallinity PET films at 30 °C. *I. sakaiensis* 201-F6 utilized PET as its primary carbon and energy source to support growth [4]. Genome analysis of *I. sakaiensis* uncovered the existence of two distinctive enzymes, PETase and MHETase, constituting an essential dual enzyme system for PET hydrolysis. The collaborative action of these enzymes is essential for effectively breaking down PET [5,6]. The initial enzyme in this system, PETase (EC 3.1.1.101) or FastPETase, functions as an esterase, catalyzing ester bonds and hydrolyzing polymerized PET molecules. As shown in Fig. S1, hydrolysis of PET results in the release of significant amounts of monomeric monohydroxyethyl terephthalate (MHET), along with smaller quantities of bishydroxyethyl terephthalate (BHET) and TPA [7,8]. As the primary intermediate product, MHET exerts a potent inhibitory effect on PET hydrolase activity [9]. MHETase (EC 3.1.1.102), a hydrolase identified in *I. sakaiensis*, can effectively break down MHET

Peer review under responsibility of KeAi Communications Co., Ltd.
* Corresponding author.
E-mail address: whzhong@zjut.edu.cn (W. Zhong).

https://doi.org/10.1016/j.synbio.2024.08.001
Received 23 June 2024; Received in revised form 30 July 2024; Accepted 2 August 2024
Available online 3 August 2024

into TPA and EG through synergy with PETase (Fig. S1), indicating that *I. sakaiensis* has evolved a distinct strategy to mitigate the impact of product inhibition [10]. The addition of MHETase in PETase reaction system accelerated PET breakdown twice as rapidly as PETase alone [11]. A chimeric two-enzyme system where MHETase is connected to PETase through glycine-serine linkers of varying lengths (8, 12, or 20 amino acid residues), showed a better degradation efficiency of amorphous PET than a mixture of PETase and MHETase [12]. To address PET pollution, enzymatic degradation technology employing PET hydrolase emerges as a safe and sustainable alternative, enabling the environmentally friendly recycling of PET [13]. In recent years, numerous PET hydrolases have been identified and characterized from various microorganisms, and been engineered to enhance their performance in practical applications [14–17]. These resulting monomers TPA and EG from PET biodegradation can undergo additional recycling processes, demonstrating a green and eco-friendly approach to PET recycling [4].

In recent years, the advancement of microbial cell surface display technology has introduced a novel approach to address the challenge of microbial degradation of PET, given inherent difficulty of PET entering cells. Cell surface display technology, a protein application method developed through recombinant DNA technology, involves expressing and localizing exogenous functional proteins on the surface of specific bacterial cells for research and practical applications [18,19]. This system comprises three essential components: anchor protein, target protein, and recipient bacterium. An appropriate anchor protein is necessary for cell surface display technology. Various anchor proteins have been employed in microbial cell surface display, including outer membrane proteins, lipoproteins, surface appendage subunits, and S-layer proteins [20–22]. Among these, outer membrane proteins are particularly favored as anchor motifs for peptide and protein display due to their efficient secretion signal, robust anchoring capabilities, and distinctive transmembrane structure which can offer fusion sites for target protein. As outer membrane proteins, OmpA, OprF, OmpS, FadL, LamB, PhoE, OmpC, and Lpp–OmpA have proven successful utilized as anchor motifs [23–25]. Additionally, co-display system has been successfully used mainly in *E. coli*, *Saccharomyces cerevisiae*, and *Pichia pastoris* [26–29].

Recently, surface display systems and whole-cell biocatalysts have been reported for the expression and functional evaluation of PET hydrolases [30,31]. By employing DNA recombination, the PET hydrolase gene is incorporated into a cell surface display expression vector. This genetic modification ensures the fixation of PET hydrolase on the microbial cell surface through anchor proteins. The resulting displayed enzyme retains high biological activity, effectively addressing challenges associated with limited direct substrate contact and activity loss during extraction processes [32]. Additionally, PETase surface display system and MHETase surface display system have been successfully constructed in yeast, and superior thermal stability and increased conversion rates compared to purified enzymes was observed [33,34].

Pseudomonas sp. JY-Q, isolated from waste tobacco aqueous extract, exhibited robust stress resistance, with a mature genetic operating system, and a downstream pathway for PET degradation from protocatechuic acid (PCA) into the TCA cycle [35,36]. Thus, *Pseudomonas* sp. JY-Q was selected as the recipient strain for cell surface display in this study. The truncated OmpA and its variants in strain JY-Q was selected as anchor motifs to construct non-tandem double-enzyme co-display strains for PETase and MHETase. In addition, FASTPETase- MHETase tandem double-enzyme co-displaying strains were created. This strategic design aimed to explore the biocatalytic potential of recombinant bacteria in displaying PET hydrolase on the cell surface.

Phthalate esters (PAEs) are a class of plasticizers widely used in plastic production, and release of PAEs cause environmental pollution because PAEs are endocrine-disrupting chemicals. Due to the widespread use of PET around the world, several studies have reported that the combined contamination of PET and PAEs is a serious environmental problem [37–39]. PAEs esterase gene was integrated into the genome of JY-Q, for final combining both PAEs and PET degrading ability in JY-Q. The esterase genes were mined from *Rhodococcus* sp. AH-ZY2 which exhibited strong degradation ability for multiple PAEs. The esterase EstR1 encoded by AH-ZY2-*estR1* has a similarity of 57.88 % with the reported carboxyesterase, and is predicted to be a type III enzyme (with high activity on phthalate diesters). The esterase EstR4 encoded by AH-ZY2-*estR4* has a sequence similarity of up to 100 % with the reported MehpH esterase, indicating that EstR4 is a mono-ethylhexylphthalate degrading esterase and belongs to type II enzyme (with high activity on phthalate monoesters). Heterologous expression of esterase genes was performed, and high performance liquid chromatography (HPLC) results showed that EstR1 and EstR4 had the function of degrading PAEs [40]. Then, AH-ZY2-*estR1* and AH-ZY2-*estR4* genes were inserted into the JY-Q genome via replacing *RS11060* and *upp* gene through homologous recombination, respectively. Finally, the resultant recombinant strain JY-Q *ΔRS11060::estR1Δupp::estR4* (JY-Q-R1-R4) can simultaneously degrade both long and short chains of PAEs to phthalic acid (PA). In this study, *sfm-6his* (encoding co-displayed tandem FASTPETase-MHETase) was integrated into the JY-Q-R1-R4 genome to obtain JY-Q-R1-R4-SFM. Moreover, gene cluster $tphA2_{II}A3_{II}B_{II}A1_{II}$ (encoding TPA 1,2- dioxygenase (TPADO) and 1,2-dihydroxy-3,5-cyclohexadiene-1,4-dicarboxylate dehydrogenase (DCDDH) responsible for transformation of TPA to PCA) was integrated to JY-Q-R1-R4-SFM to construct JY-Q-R1-R4-SFM-TPH, aiming to obtain a strain that can degrade PET or BHET completely. Ability of these engineered strains to degrade PET and PAEs combined pollution was investigated (Fig. 1).

2. Materials and methods

2.1. Media

LB medium composition (per liter): 10.00 g peptone, 5.00 g yeast extract, 10.00 g sodium chloride (NaCl).

BSM medium composition (per liter): 5.57 g sodium phosphate dibasic (Na_2HPO_4), 2.44 g potassium phosphate monobasic (KH_2PO_4), 1.00 g potassium sulfate (K_2SO_4), 0.20 g magnesium chloride ($MgCl_2{\bullet}6H_2O$), 1.00 mg calcium chloride ($CaCl_2$), 1.00 mg iron chloride ($FeCl_3{\bullet}6H_2O$), 0.40 mg manganese chloride ($MnCl_2{\bullet}4H_2O$).

Nicotine-supplemented BSM medium: prepare BSM medium and add 2 g/L nicotine, adjusting the pH to 7.

2.2. Strains and plasmids

Strains and plasmids used in this study are listed in Table 1.

Escherichia coli DH5α served as the host for plasmid cloning, while *Pseudomonas* sp. JY-Q functioned as the recipient bacteria for expression and surface display. Cultures of *E. coli* DH5α and its recombinant strain were grown on LB plates or in LB liquid medium using flasks at 37 °C with agitation at 180 rpm. Strain JY-Q and its recombinant strains were cultivated in LB medium or nicotine-supplemented BSM.

Table 2 presents a comprehensive list of all genes utilized in this study. The *petase* gene, derived from *I. sakaiensis* 201-F6, underwent codon optimization and synthesis by BGI. Similarly, *mhetase* and *fastpetase* were codon-optimized and synthesized by Tsingke Biotech. The primers used throughout the study were synthesized by Tsingke Biotech and are detailed in Table 3. High-fidelity DNA polymerase was purchased from Nanjing Vazyme Bio Co., Ltd., while the restriction enzyme was obtained from TaKaRa (TaKaRaBio). Genome extraction kits, RNA extraction kits, and reverse transcription kits were purchased from Jiangsu CWBIO Biotechnology. Standards for BHET, MHET, TPA dibutyl phthalate (DBP), bis(2-ethylhexyl) phthalate (DEHP) and phthalic acid (PA) were acquired from Aladdin, and all other chemical reagents were purchased from Sangon Biotech.

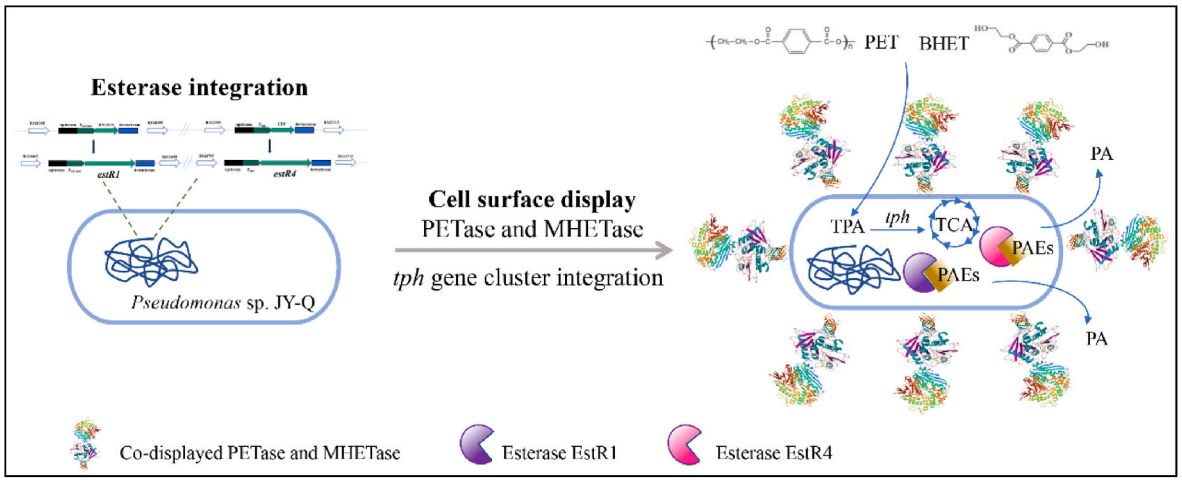

Fig. 1. Schematic of engineering of PETase-MHETase surface-co-displayed systems in esterase-integrated *Pseudomonas* sp. JY-Q.

2.3. High performance liquid chromatography analysis

HPLC was employed to assess the variations in BHET, MHET, and TPA. A mixture of 100 μL of the supernatant sample and 300 μL of a 20 mM phosphate-buffered saline solution (PBS) with a pH of 2.50 (containing 20 % dimethyl sulfoxide) was prepared and subsequently filtered through a 0.22 μm filter membrane. The analysis was carried out using liquid chromatography on ZORBAX Eclipse XDB-C18 (4.60 mm × 250 mm). The mobile phase consisted of 50 % (*v/v*) chromatographed methanol and 50 % (*v/v*) 20 mM PBS (pH = 2.50) a flow rate of 1 mL/min. Detection was performed at a wavelength of 245 nm, with a detection time of 7 min and an injection volume of 10 μL. The detection of DBP, DEHP and PA was according to previous study [40].

2.4. Confocal microscopy and fluorescence microscopy analysis

Both confocal microscopy and inverted fluorescence microscopy serve as tools for observing the fluorescence of strain cells. Confocal microscopy allows for a layered examination of cells. The recombinant plasmid was introduced into strain JY-Q through electroporation, followed by plating on LB plates supplemented with ampicillin. The plated samples were then incubated overnight at 37 °C. Single colonies were chosen for validation and inoculated in ampicillin-containing LB medium. The culture was incubated on a shaker at 180 rpm until reaching an OD_{600} of 0.6–0.8. Initially, the culture was maintained at 22 °C and 180 rpm for 30 min before induction by adding 1 mM IPTG. Following induction, *E. coli* was cultured at a low temperature for 16–18 h, and *Pseudomonas* sp. JY-Q was cultured at a low temperature for 24 h. The bacterial culture was washed three times with 1 × PBS, and the samples were then prepared for microscopic observation. The prepared slides were placed under a laser scanning confocal microscope STELLARIS STED (Leica) and an inverted fluorescence microscope EVOS M5000 (Thermo Fisher Scientific). The focal length was adjusted, and the fluorescence patterns and positions were observed before capturing photographs for documentation.

2.5. PET film degradation and field emission scanning electron microscopy analysis

The PET film underwent cutting into 2 cm × 2 cm squares and received pre-treatment according to previous study [41]. Recombinant bacteria were cultured, collected, and concentrated through centrifugation, then pipetted onto PET membranes that had undergone pre-treatment. These reaction mixtures were left to incubate in a water bath at 30 °C for a duration of 28 days, during which the bacterial solution was changed weekly. Following the 28-day incubation period, the PET film was removed, washed, and dried in a 60 °C oven. The blank control group underwent treatment with an equivalent volume of BSM medium. Subsequently, the washed and dried PET film sample underwent surface metallization in an ion sputtering coater and was then examined and imaged using a scanning electron microscope.

2.6. Indirect immunofluorescence assays

Initially, the OD_{600} of both the negative control group samples and experimental group samples was carefully maintained between 0.4 and 0.6. Then, the samples were treated with 4 % paraformaldehyde for 10 min at room temperature to facilitate cell fixation. Next, the samples were washed twice with pre-chilled sterilized PBS and resuspended with 200 μL of primary antibody dilution, and incubated overnight in a 4 °C freezer. The next day, the samples were removed from the refrigerator and left at room temperature for 10 min before being washed three times with sterilized PBS. 200 μL of secondary antibody reagent was added to the samples and incubated at 37 °C for 1 h in the dark. Finally, the samples were washed twice with sterilized PBS and prepared for observation. Prior to mounting, slides and coverslips were picked up with tweezers and immersed in a beaker filled with 90 % ethanol, where the slides were washed with ethanol.

2.7. AlphaFold 2 modeling

The AlphaFold2 AI system, developed by DeepMind, has the capability to directly generate structural models of protein-protein complexes based on sequence information. A significant portion of the prediction models align closely with experimental protein structure models [42]. An index, pLDDT, was introduced to assess the reliability of monomer structure predicted by AlphaFold2. This index ranges from 0 to 100, with higher value indicating greater confidence in the prediction model. In this study, AlphaFold2 software was employed to predict the following complexes: anchor protein, anchor protein-linker-PETase, anchor protein-linker-MHETase, and FASTPETase-MHETase.

2.8. Degradation test

Cells were cultivated overnight in LB medium supplemented corresponding antibiotics, then collected by centrifugation and washes three times with sterilized PBS. The collected cells were then resuspended with PBS. Either 4 g of pre-treated PET powder or 200 mg/L of BHET and MHET were introduced to the cell suspension. The reaction mixtures were incubated at 30 °C, and the supernatant was periodically sampled. The changes in substrate consumption and product formation were

Table 1
Strains and plasmids used in this study.

Strain and plasmid	Characteristic	Source
Strain		
Pseudomonas sp. JY-Q	Wild type	Lab stock
JY-Q/p519n-*petase-his*	p519n-*petase-his* in JY-Q	This study
JY-Q/pMMB67EH-*signal (oprF)-cOpma-gfp*	pMMB67EH-*signal(oprF)-cOpma-gfp* in JY-Q	This study
JY-Q/p519n-*signal(oprF)-cOpma-petase-his*	p519n-*signal(oprF)-cOpma-petase-his* in JY-Q	This study
JY-Q/pMMB67EH-*cOpma-gfp*	pMMB67EH-*cOpma-gfp* in JY-Q	This study
JY-Q/p519n-*cOpma-petase-his*	p519n-*cOpma-petase-his* in JY-Q	This study
JY-Q/p519n-*signal(oprF)-cOmpa-petase-his*	JY-Q containing recombinant plasmid for surface display	Lab stock
E. coli DH5α	Host to replicate plasmids	This study
E. coli DH5α/pK18*mobsacB*	pK18*mobsacB* integrated plasmid clone host	This study
E.coli DH5α/pK18*mobsacBΔRS09985::SOP-his*	pK18*mobsacBΔRS09985::SOP-his* clone host	This study
E. coli WM3064	2,6-DAP trophic deficient strain	This study
WM3064/ pK18*mobsacBΔRS09985::SOP-his*	pK18*mobsacBΔRS09985::SOP-his* donor bacteria	This study
JY-Q/p519n-*mhetase-his*	p519n-*mhetase-his* in JY-Q	This study
JY-Q/p519n-*so-mhetase-flag*	p519n-*so-mhetase-flag* in JY-Q	This study
JY-QΔ*RS09985::SOP-his*/ p519n-*SOM-flag*	p519n-*signal(oprF)-cOmpa-mhetase-flag* in JY-QΔ*RS09985::SOP-his*	This study
JY-Q/p519n-*SOF*	p519n-*signal(oprF)-cOmpa-fastpetase-flag* in JY-Q	This study
JY-Q/p519n-*SOFM-his*	p519n-signal(oprF)-cOmpa-fastpetase-mhetase-6his in JY-Q	This study
JY-Q-R1-R4	JY-QΔ*RS11060::estR1*Δ*upp::estR4*	This study
JY-Q-R1-R4-SFM	JY-QΔ*RS09985::estR1*Δ*upp::estR4*: *sfm-6his*	This study
JY-Q-R1-R4-SFM-TPH	Integrate gene cluster *PRS09985tphA2*ΙΙ*A3*ΙΙ*B*ΙΙ*A1*ΙΙ at the intergenic region between RS14415 and RS14420 in strain JY-Q-R1-R4-SFM	This study
Plasmid		
pMMB67EH-*signal(oprF)-compa-gfp*	p519n carries fusion protein formed by *signal(oprF)-compa* and *petase-his*	This study
p519n-*signal(oprF)-compa-petase-his*	p519n carries fusion protein formed by *signal(oprF)-compa* and *petase-his*	This study
pMMB67EH-*cOmpa-gfp*	pMMB67EH carries a fusion protein formed by truncating the combination of *ompa* and *gfp*	This study
p519n-*cOmpa-petase-his*	p519n carries a fusion protein that combines truncated *ompa* and *petase-his*	This study
pK18*mobsacB*	Integrated plasmid, sacB、KmR genes	This study
pK18*mobsacBΔRS09985::SOP-his*	pK18*mbobsacB* with *SOP-his* gene	This study
p519n-*gfp*	Expression plasmid	Agricultura University
p519n-*mhetase-his*	*mhetase-6his* in p519n-*gfp*	This study
p519n-*signal(oprF)-cOmpa-mhetase*	p519n carries fusion protein formed by the anchor protein and *mhetase-flag*	This study
p519n-*signal(oprF)-cOmpa-fastpetase-flag*	p519 carries fusion protein formed by the anchor protein and *fas-flag tpetase-flag*	This study
p519n-*signal(oprF)-cOmpa-fastpetase-mhetase-his*	p519 carries fusion protein formed by the anchor protein and *fastpetase-mhetase-his*	This study
p519n-*fastpetase-mhetase-his*	p519 carries fusion protein formed by the *fastpetase-mhetase-his*	This study

Table 2
List of genes used in this study.

Gene names	Source organism	Accession numbers
petase	*I. sakaiensis*	OR020853
mhetase	*I. sakaiensis*	ORO20854
fastpetase	*I. sakaiensis*	OR020855

assessed and quantified using high-performance liquid chromatography Agilent 1260 (Agilent).

2.9. Biodegradation of combined pollutants of polyethylene terephthalate and phthalate esters by JY-Q-R1-R4-SFM and JY-Q-R1-R4-SFM-TPH

Sfm-6his (encoding cell surface displayed FASTPETase and MHETase, amplified from plasmid p519n-*signal(oprF)-cOmpa-fastpetase-mhetase-his*) was integrated into the genome of the strain JY-Q-R1-R4 to obtain JY-Q-R1-R4-SFM. To achieve a complete degradation of PET and BHET by JY-Q-R1-R4-SFM, TPA degradation gene clusters, $tphA2_{II}A3_{II}B_{II}A1_{II}$, from strain *Comamonas* sp. strain E6 [43] were synthesized and integrated into JY-Q-R1-R4-SFM to obtain JY-Q-R1-R4-SFM-TPH. Ability of JY-Q-R1-R4-SFM and JY-Q-R1-R4-SFM-TPH to degrade PET and PAEs combined pollution was investigated. Strains were inoculated into 5 mL LB liquid medium and cultured overnight at 37 °C, 180 rpm, and 2 % overnight culture were transferred to 100 mL fresh LB liquid medium and incubated until the OD_{600} reach to 0.6–0.8 (mid-log phase), respectively. Cells were collected by centrifugation at 5000 rpm for 5 min, obtaining pellets were washed with PBS twice and resuspended to obtain a cell suspension with $OD_{600} = 10$. The cell suspensions were used to detect its ability to transform BHET and DBP. The initial concentration of BHET and DBP was both 200 mg/L. DBP was used because it is one of the most commonly used PAEs in PET production. Cell suspension of strain JY-Q-R1-R4-SFM and JY-Q-R1-R4-SFM-TPH were used as experimental group, cell suspensions of JY-Q-R1-R4 and wild-type JY-Q were used as control group, and group without cell suspension was set as the negative control. Each group was conducted three parallel repeats, the substrate consumption and product formation were detected after being cultured at 37 °C for 16, 48 and 72 h.

Additionally, PET film and a mixture of DBP and DEHP (DBP is a typical short-chain PAEs and DEHP is a typical long-chain PAEs) were treated by JY-Q-R1-R4-SFM-TPH, JY-Q-R1-R4-SFM, and JY-Q-R1-R4, meanwhile a group that treated by wild-type JY-Q was used as control strain, and another group that treated by no strain with PBS containing substrate only was used as negative control group. PET films were pretreated and incubated with cell suspensions for 28 days before detection by a Hitachi S-4700 (Hitachi) for SEM analysis. DBP and DEHP were detected by HPLC after incubation for 16 h.

2.10. Data analysis

Data are expressed as means ± standard deviations of a representative of three similar experiments carried out in triplicate. Statistical analysis (mean, standard deviation) and drawing were performed using Graphpad Prism 9 (GraphPad Software, Boston, Massachusetts USA, www.graphpad.com).

3. Results

3.1. Construction of a surface display system in JY-Q

The frequently utilized anchor protein, Outer membrane protein A (OmpA), was shown in Fig. S2. OmpA from *Escherichia coli* has 8 transmembrane regions and periplasmic N-terminal and C-terminal. OmpA forms three inner ring structures and four outer ring structures, and the outer ring can be served as the insertion site for proteins requiring surface display [44,45]. Analysis results of the genome of

Table 3
Primers used in this study.

Primer name	Sequences (5'to 3')
Fragment cloning	
signal(oprf)-copma-gfp s F	CGGGGATCCTCTAGAGTCGACATGAAACT
signal(oprf)-copma-gfp s R	GAAGAACACCTTAGGCGCGGCGCCTTGGCCCTGGGCAAAGG
signal(oprf)-copma-gfp o F	TGCCCAGGGCCAAGGCGCCGTCGAG
signal(oprf)-copma-gfp o R	CTCCTGATCCACCTCCACCTGATCCACCTCC
signal(oprf)-copma-gfp g F	ACCGCCCTGGTCGATGTTGTACTAGGTGGAGGTGGATCAGGAGGTGGAGGATCAATGAGTAAAGGAGAAGAACTTT
signal(oprf)-copma-gfp g R	TCCGCCAAAACAGCCAAGCTTTTATTTGTATAGTTCATCCATGCCATGTGTAATCC
copma-gfp o F	CCCGGGGATCCTCTAGAGTCGACATGAAA
copma-gfp o R	TTGAAAAACACCTTGGGCTTGATCCACCTCCACCTGATCCACCTCCACCGCCCTGGTCGATGTTGTACTGAG
copma-gfp g F	GTGGATCAGGTGGAGGTGGATCAGGAGGTGGAGGATCAATGAGTAAAGGAGAAGAA
copma-gfp g R	CATCCGCCAAAACAGCCAAGCTTTTATTTGTATAGTTCATCCATGCCATGTGTAATCC
signal(oprf)-copma-petase s F	GATCTGATGGCGCTCTAGAATGAAACTGAAGAACACCTTAGGCGTTGTCATCG
signal(oprf)-copma-petase s R	CGGCGCCTTGGCCCTGGGCAAAGG
signal(oprf)-copma-petase o F	TGCCCAGGGCCAAGGCGCCGTCGAG
signal(oprf)-copma-petase o R	GAAATTCATTGATCCTCCACCTCCTGATCCACCTCCACCT
signal(oprf)-copma-petase p F	GGAGGATCAATGAATTTCCCGCGTGCCAGCC
signal(oprf)-copma-petase p R	AACGACGGCCAGTGAATTCTTAGCTACAATTGGCAGTACGGAAGTCGCTCAC
copma-petase o F	GATCTGATGGCGCTCTAGAATGAAATTGAAAAACACCTTGGGCTTGGCCA
copma-petase o R	GAAATTCATTGATCCTCCACCTCCTGATCCACCTCCACCT
copma-petase p F	GGAGGATCAATGAATTTCCCGCGTGCCAGCC
copma-petase p R	AACGACGGCCAGTGAATTCTTAGCTACAATTGGCAGTACGGAAGTCGCTCAC
petase F	AGGATCTGATGGCGCTCTAGAATGAATTTCCCGCGTGCC
petase R	AAAACGACGGCCAGTGAATTCTTAGCTACAATTGGCAGTACGGAAGT
petase-6his F	AGGATCTGATGGCGCTCTAGAATGAATTTCCCGCGTGCC
petase-6his R	AACGACGGCCAGTGAATTCTTAATGATGATGATGATGATGGCTACAATTGGC
SOM-fiag s R	GGTCACGGTGGTCTGCATTGATVVTCCACCTCCTGATC
SOM-flag m F	GGTGGATCAGGAGGTGGAGGATCAATGCAGACCACCGTGACCACC
SOM-flag m R	AAACGACGGCCAGTGAATTCTTGTCATCGTCGTCCTTGTAATCTCACGGGGGGGCGGCGCAG
S-SF.FOR	TAGGATCTGATGGCGCTCTAGATGAAACTGAAGAACACCTTAGGCG
S-SF.REV	GGGCGTACGGGTTGGTCTGTGATCCTCCACCTCCTGATCCA
F-SF.FOR	ATCAGGAGGTGGAGGATCACAGACCAACCCGTACGCC
F-SF.REV	AACGACGGCCAGTGAATTCTTGTCGTCGTCGTCTTTGTAGT
M-SOFM.FOR	GCCAATTGCAGCCTGGAGGGTGGAGGTGGATCAGGT
M-SOFM.REV	AACGACGGCCAGTGAATTATGATGATGATGATGATGTCACGGG
SF-SOFM.FOR	GGATCTGATGGCGCTCTAGATGAAACTGAAGAACACCTT
SF-SOFM.REV	ACCTGATCCACCTCCACCCTCCAGGCTGCAATTGG
p519-FM-his.FOR	GATCTGATGGCGCTCTAGCAGACCAACCCGTACGCC
sfm-6his-UF	TCGGTACCCGGGGATCCGCTCCTGCGAAATGATTT
sfm-6his-UR	GTGAGCCAGTGAGAACCACTACTCCT
sfm-6his-F	GGGGAACACATGAAACTGAAGAACACCTTAGGCG
sfm-6his-R	TAGAGTGTCTCCTTATCACGGGGGGCGGCG
sfm-6his-DF	CCCCCCCGTGATAAGGAGACACTCTAGTAGTGACGTATGA
sfm-6his-DR	GACGGCCAGTGCCAAGCTTCGATTCACCAAACCTTCGAAAAATCAATACA
sfm-6his-PF	CAGTGAGAACACTACTCCTCGCAGGTCTTCT
sfm-6his-PR	GGTGTTCTTCAGTTTCATGTGTTCCCCTTCAAGGACTTTCTA
pK18-F	AGCTTGGCACTGGCCGTCGTT
pK18-R	GATCCCCGGGTACCGAGCTC
Q(sfm-6his)-F	TTCATTACCTGACAGGAAGGATA
Q(sfm-6his)-R	GGAATTTCTCAAGTAAATCGCTAGC
Q(sfm-6his)-UF	CTTTGATTATGCAGAACTCATTG
Q(sfm-6his)-DR	AGCTCGGGAGGTTTTGATATCTAC
tph-UF	TGACCATGATTACGAATTCAGCAAGCTGCGGCCG
tph-UR	CCTGCGAGGAGTAGTGGCCGGGTTTTTCCAATCGC
tph-F	TTGAAGGGGAACACGATGCAGGAGTCGATCATCCAGT
tph-R	TGAGATATTTGTAGATTAGTGGTGCCCGGTCGG
tph-DF	GTCCTTGAAGGGGAACACGTCTACAAATATCTCATGCTTTATTTTCAC
tph-DR	CCTGCAGGTCGACTCTAGATTTGGAGAGATCTCATTGG
tph-PF	TTGGAAAAACCCGGCCACTACTCCTCGCAGGTCTTCT
tph-PR	GCATGAGATATTTGTAGACGTGTTCCCCTTCAAGGACTT
M13-F	CAGGAAACAGCTATGAC
M13-R	GTAAAACGACGGCCAGT

Pseudomonas sp. JY-Q (NZ_CP011525) deposited in NCBI revealed 10 OmpA proteins. The OmpA protein in Pseudomonas sp. JY-Q exhibited high sequence similarity to the previously reported outer membrane protein used in the cell surface systems of other Pseudomonas strains. This study used OmpA protein (WP_003248667.1) in JY-Q, composed of 344 amino acids and with a molecular weight of 37.0 kDa, as the anchor protein. The protein's model was generated using AlphaFold2, and Fig. S2 illustrates the three-dimensional structural diagram of OmpA. As a non-specific channel protein, OmpA allows the passage of small hydrophiles and plays a structural role in maintaining cell shape and outer membrane integrity.

In theory, all four outer loops of OmpA could potentially serve as the insertion site for the target protein for cell surface display. However, previous studies indicated that the outer loop of OmpA had specific requirements on the molecular weight and charge of the inserted protein. Seung et al. achieved successful surface display of lipase using the truncated outer membrane protein OprF in *Pseudomonas aeruginosa* as an anchor motif [23]. Alignment analysis revealed that the conserved domain of OprF protein was identical to that of the outer membrane OmpA (WP_003248667.1) in JY-Q. To improve the capacity of OmpA to

receive exogenous inserted protein and reach a successful protein surface display, OmpA underwent truncation and a truncated OmpA designated as cOmpA was constructed. The target protein was inserted into the fourth loop of cOmpA, enabling the surface display of the enzyme. Considering the essential role of the signal peptide in display efficiency, the signal peptide of truncated cOmpA was replaced with the signal peptide of OprF, resulting in Signal(OprF)-cOmpA, which was also employed as the surface-displayed anchor protein.

3.2. Verification of the surface display system in JY-Q

The performance of cOmpA and Signal(OprF)-cOmpA were determined by reporter gene. Fluorescent proteins, such as GFP, serve as valuable reporter genes for detecting gene expression, regulation, and fusion tags, enabling the observation of localization, migration, and conformational changes in protein molecules. In this study, the green fluorescent protein gene, gfp (derived from plasmid p519n-gfp), was employed as the reporter gene to construct cOmpA-gfp and Signal (OprF)-cOmpA-gfp. These two fusion genes were ligated into the expression vector pMMB67EH (digested by *Sal*I and *Hin*dIII) to obtain pMMB67EH-cOmpA-gfp and pMMB67EH-Signal(OprF)-cOmpA-gfp, respectively. These two resulting plasmids were imported to JY-Q to obtain JY-Q/pMMB67EH-Signal(OprF)-cOmpA-gfp and JY-Q/pMMB67EH- cOmpA-gfp. These two recombinant bacteria were cultured and underwent induction with IPTG at low-temperature for 24 h, and then fluorescence was observed using inverted fluorescence microscopy and confocal microscopy. Under inverted fluorescence microscopy, green fluorescence was evident in both JY-Q/pMMB67EH-Signal (OprF)-cOmpA-gfp and JY-Q/pMMB67EH-cOmpA-gfp strains. The fluorescence distribution in JY-Q/pMMB67EH- Signal(OprF)-cOmpA-gfp appeared more uniform compared to JY-Q/pMMB67EH-cOmpA-gfp when observed by confocal microscopy (Fig. 2). In a previous study, Lpp-OmpA was utilized as an anchor protein, and an immune response was employed to identify the location of the target protein. Results showed that fluorescence could be observed in various regions around the periphery of bacteria, which indicated the successfully display of target protein by Lpp-OmpA [46]. Gallus et al. also utilized the anchor protein Lpp-OmpA for displaying the target protein on the surface of *E. coli*. In bacteria carrying the Lpp-OmpA-GFP protein, fluorescence was observed at the cell periphery under the microscope [20]. The fluorescence distribution of the fusion protein cOmpA-GFP and Signal (OprF)-cOmpA-GFP were similar with that in previous study, which indicated that the surface display system was constructed successful in JY-Q.

3.3. Heterologous expression and enzyme activity determination of PETase and MHETase in Pseudomonas sp. JY-Q

In this investigation, the *petase* and *mhetase* genes from *I. sakaiensis* 201-F6 underwent codon optimization before being introduced to JY-Q. The constitutive expression plasmid p519n-gfp was digested with *Xba*I and *Eco*RI, and the green fluorescent protein gene on the plasmid was replaced with the target gene (*petase* and *mhetase* carrying His-tag). Then the obtaining expression vectors p519n-*petase-6his* and p519n-*mhetase-6his* were transformed into JY-Q, generating JY-Q/p519n-*petase-6his* and JY-Q/p519n-*mhetase-6his*. The resultant strains were cultured, then cells were harvested and broken by an ultrasonic cell disruptor to obtain crude enzyme solutions. Further purification involved nickel column purification and gradient elution with imidazole was implemented to yield purified PETase and MHETase. The protein concentration of both crude and purified enzyme solutions was determined by BCA method. Sodium dodecyl sulfate-polyacrylamide gel electrophoresis (SDS-PAGE) was used to analyze the purified protein. SDS-PAGE results confirmed the successful isolation of purification of PETase-His protein (Fig. 3A, lane 4) and MHETase-His protein (Fig. 3B, lane 13). The size of the recombinant protein was accordance with theoretically calculated molecular weights of 31.0 kDa for PETase-His and 65.3 kDa for MHETase-His, respectively. Enzyme activity assays for both crude and pure enzyme of PETase and MHETase were performed. HPLC was used to detect substrate and product changes during enzyme reaction system. PETase can hydrolyze ester bonds in PET, breakdown PET into small molecules such as BHET, MHET, and TPA. In order to detect the substrate consumption more conveniently, BHET was used as the substrate of PETase. Results showed that PETas-His can catalyze BHET to produce MHET and TPA (Fig. 3C). The data demonstrated the activity of the PETase synthesized in this study. In the MHET degradation assay, both the crude and pure enzyme solutions of MHETase efficiently degraded MHET, leading to the formation of TPA (Fig. 3D). These results indicated that the codon-optimized MHETase could be heterologously expressed in JY-Q and possessed catalytic activity.

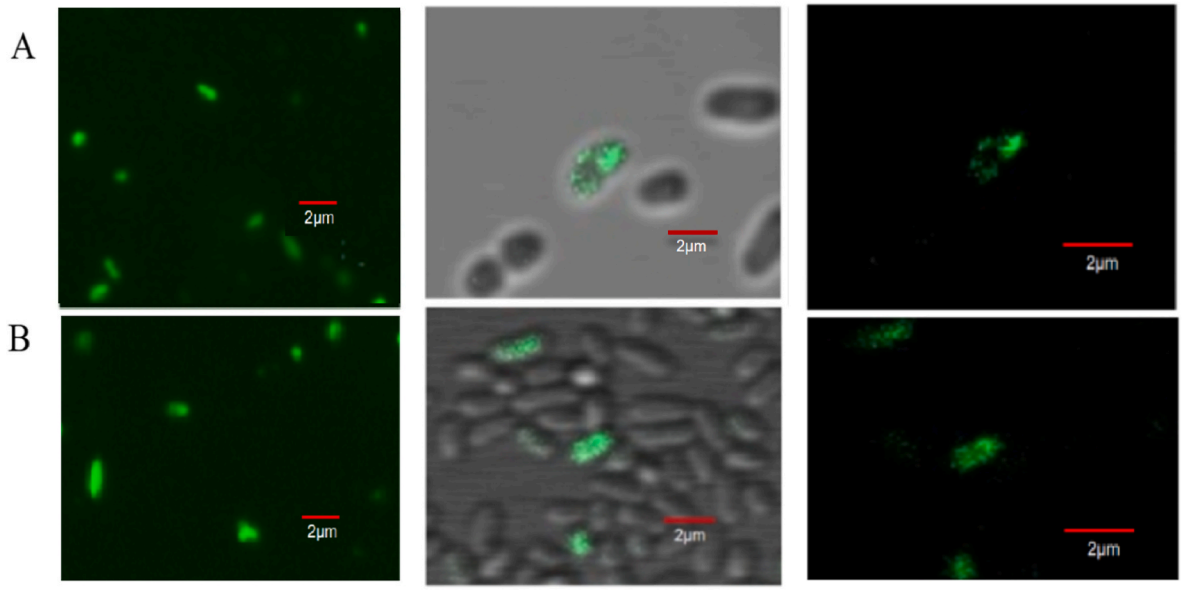

Fig. 2. Observation of GFP by inverted fluorescence microscopy and confocal microscope (from left to right are inverted fluorescence microscopy, confocal microscope light and dark field superposition and confocal microscope dark field) of two strains. (A) JY-Q/pMMB67EH-*cOpma-gfp*, (B) JY-Q/pMMB67EH-*signal(oprF)-cOmpa-gfp*.

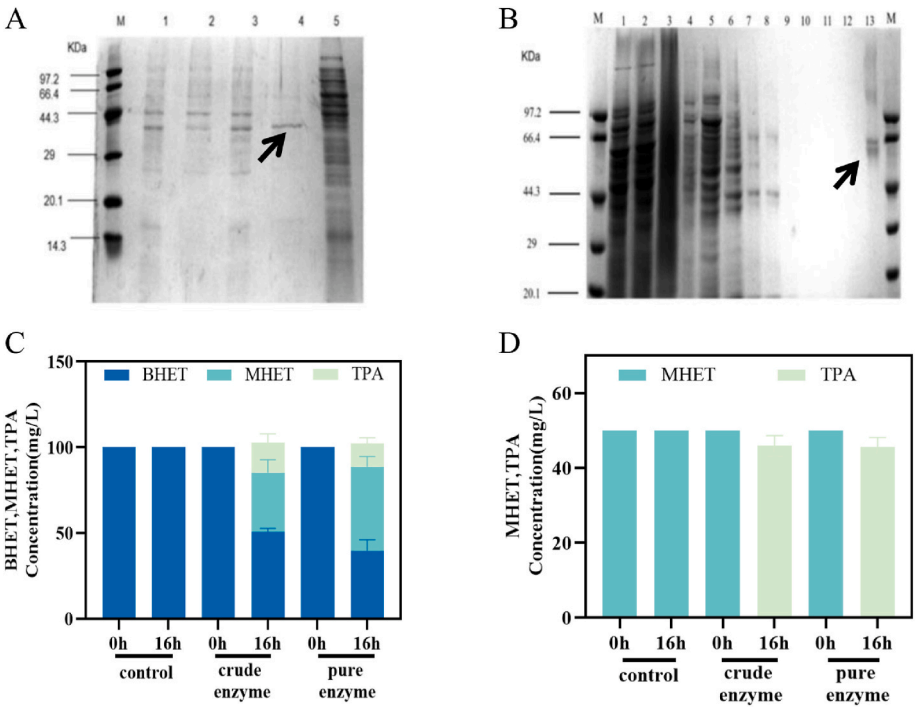

Fig. 3. Enzymatic activity identification of PETase from JY-Q/p519n-petase-6his and MHETase from JY-Q/p519n-mhetase-6his. (A) Analysis of expression and purification of PETase-His, lanes 1–5 are: 50 mM, 100 mM, 150 mM, 200 mM, and 250 mM imidazole eluent, respectively. (B) Analysis of expression and purification of MHETase-His, lanes 1–10 are: whole cell, supernatant, sediment, nickel column effluent, and 10 mM, 30 mM, 60 mM, 80 mM, 100 mM, 120 mM, 150 mM, 200 mM, 250 mM imidazole elution, respectively. (C) BHET degradation by crude PETase-His enzyme and purified PETase-His enzyme. (D) MHET degradation by crude MHETase-His enzyme and purified MHETase-His enzyme.

3.4. PETase and MHETase displayed on the surface of Pseudomonas sp. JY-Q

For the surface display of PETase in JY-Q, a recombinant plasmid p519n-*signal(oprF)- cOmpa-petase*, abbreviated as p519n-SOP-his, was engineered by combining the anchor protein *signal(oprF)-cOmpa* gene sequence with the *petase-his* gene sequence into the expression plasmid p519n-gfp. The resulting recombinant plasmid was introduced into *Pseudomonas* sp. JY-Q by electroporation, yielding the single-enzyme display strain JY-Q/p519n-*SOP-his*. PET and BHET degradation

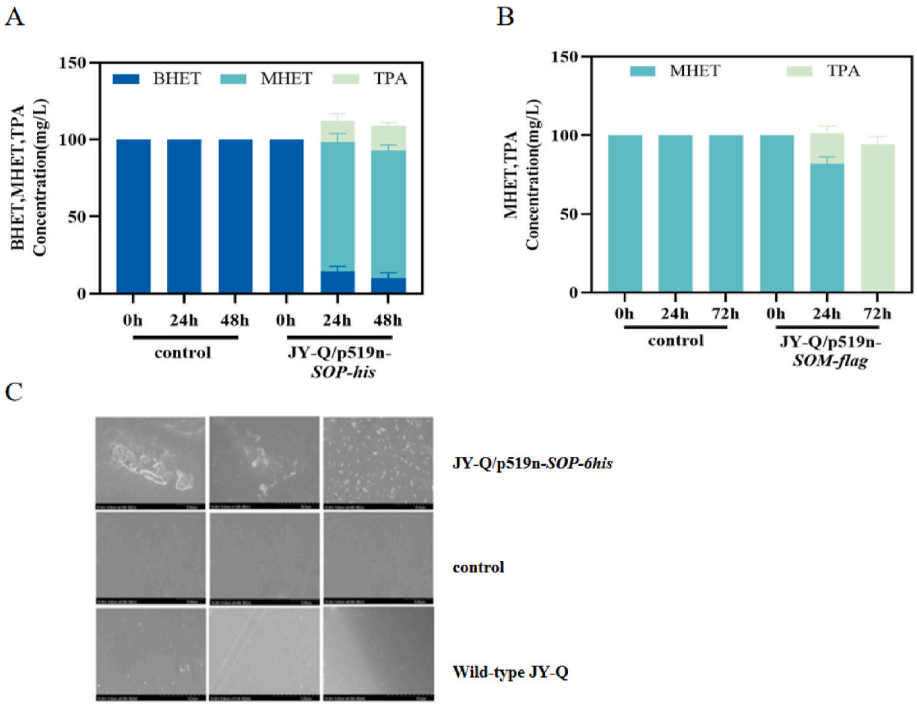

Fig. 4. Assessment of degradation performance of single enzyme displayed strains. (A) Determination of BHET degradation by JY-Q/p519n-*SOP-his*. (B) Assessment of MHET degradation effect by JY-Q/p519n-*SOM-flag*. (C) Processing effect of JY-Q/p519n-*SOP-his* on PET film observed by SEM.

experiments were conducted by JY-Q/p519n-*SOP-his* to test its performance.

The BHET degradation experiments conducted on the single-enzyme display strain JY-Q/p519n-*SOP-his* (Fig. 4A) revealed the catalytic activity of the PETase displayed on the surface of *Pseudomonas* sp. JY-Q. The enzyme efficiently degraded BHET, producing MHET and TPA as products. PET film degradation experiments were carried out using the JY-Q/p519n-*SOP-his* strain, and the results of scanning electron microscope (SEM) showed noticeable damage to the PET films after treatment with the JY-Q/p519n-*SOP-his* recombinant strain (Fig. 4C). In summary, these findings demonstrated that the surface displayed PETase exhibited catalytic activity in JY-Q cells. JY-Q/p519n-*SOP-his* can effectively degrade PET and serves as the initial PET degradation module in the co-display system.

The recombinant plasmid p519n-*signal(oprF)-cOmpa-mhetase-flag*, created by ligating the *signal(oprF)-cOmpa* sequence (encoding anchor protein) and *mhetase-flag* sequence (encoding MHETase with a Flag-tag in the C-terminal) into the expression plasmid p519n-gfp, was designed for the purpose of showcasing MHETase on the cell surface of JY-Q. The plasmid was introduced into *Pseudomonas* sp. JY-Q by electroporation, resulting in the MHETase single enzyme display strain JY-Q/p519n-*SOM-flag*. MHET degradation experiments demonstrated that 100 mg/L of MHET was entirely degraded to TPA by JY-Q/p519n-*SOM-flag* (Fig. 4B). This indicates that the MHETase displayed on the surface of JY-Q cells exhibits catalytic activity and can be incorporated into the co-display system as the second PET degradation module.

3.5. Dual-enzyme display system construction and the cell surface display verification

Two distinct construction strategies were employed to achieve the co-display of two enzymes on the cell surface of JY-Q. The first one was constructing a non-tandem two-enzyme co-display strain and the second one was constructing a tandem two-enzyme co-display strain.

For the construction of the non-tandem two-enzyme co-display strain, PETase and MHETase encoding genes were designed to integrate into genome of JY-Q or insert into a self-replicable plasmid. The integration site selection was based on genomic and transcriptome data of strain JY-Q. The FPKM value of the gene *RS09985*, encoding a hypothetical protein, was higher than other genes in both the glucose and nicotine culture groups. This indicated that the endogenous promoter $P_{RS09985}$ was stronger than other promoters, thereby capable of enhancing the expression of target genes. Consequently, the gene *RS09985*, controlled by the robust promoter $P_{RS09985}$, was chosen as the gene replacement site. The fusion gene *signal(oprF)-cOmpa-petase-his*, designated as *SOP-his*, was integrated into the JY-Q genome using *sacB* counter-selection. The resultant recombinant strain, JY-QΔ*RS09985::SOP-his*, was obtained to display PETase on the cell surface. The BHET degradation experiment (Fig. 5A) showed that *SOP-6his* driven by the robust endogenous promoter of JY-Q exhibited catalytic activity.

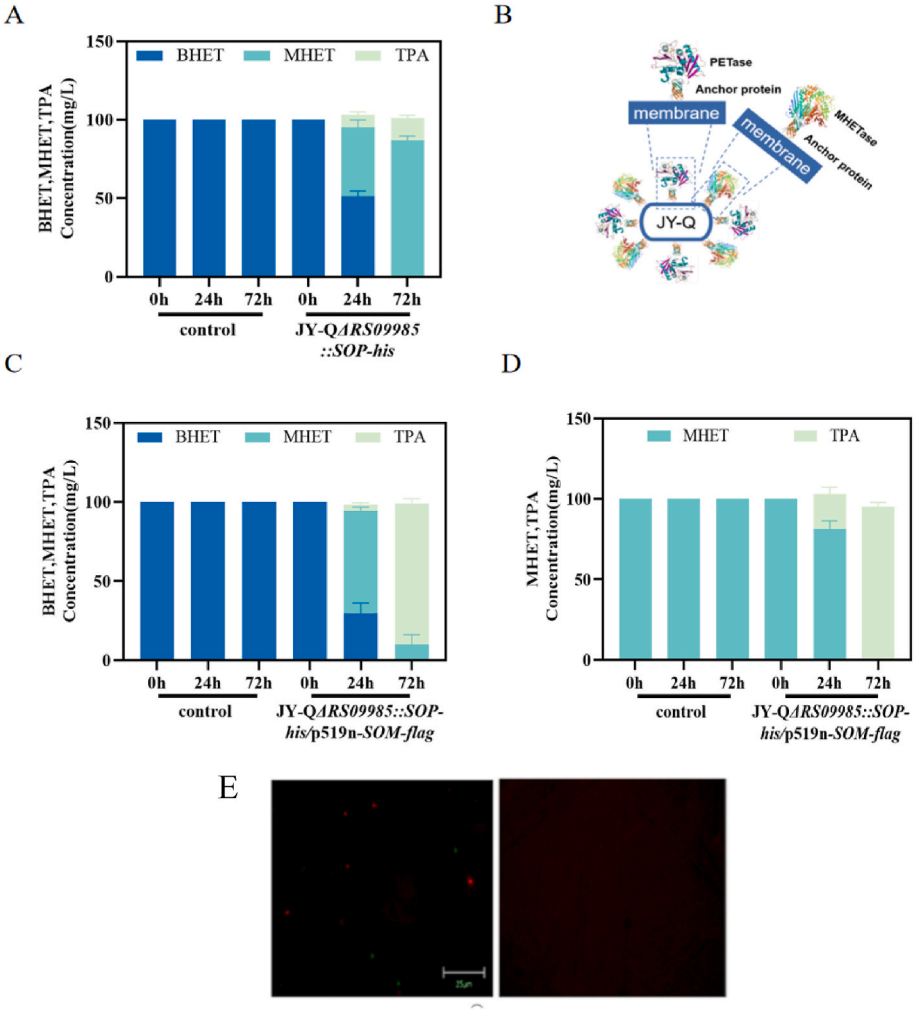

Fig. 5. Determination of the degradation performance of non-tandem double-enzyme co-display strains. (A) BHET degradation by JY-QΔ*RS09985::SOP-his*; (B) Schematic diagram of non-tandem double-enzyme co-display; (C) BHET degradation by JY-QΔ*RS09985::SOP-his/p519n-SOM-flag*; (D) MHET degradation by JY-QΔ*RS09985::SOP-his/p519n-SOM-flag*; (E) Indirect immunofluorescence mapping of non-tandem double enzyme co-display strain and control.

The non-tandem double-enzyme co-display strain, JY-QΔ*RS09985::SOP-his/p519n-SOM-flag*, was generated by introducing the MHETase display plasmid p519n-*SOM-flag* into the recombinant strain JY-QΔ*RS09985::SOP-his*. BHET and MHET degradation experiments revealed that JY-QΔ*RS09985::SOP-his/p519n-SOM-flag* exhibited catalytic activity of both PETase (Fig. 5C) and MHETase (Fig. 5D). To further confirm the successful display of PETase and MHETase on the cell surface of JY-Q, an indirect immunofluorescence localization verification was conducted. PETase, as the first enzyme displayed on the surface, carried a His-tag that bound to a primary mouse anti-His antibody. Subsequently, it was treated with a green-fluorescently labeled anti-mouse antibody (secondary antibody), causing the cells to fluoresce green under a microscope. The MHETase, harboring a Flag tag at its C-terminus, was targeted using a primary rabbit anti-Flag antibody. After treatment with a secondary anti-rabbit antibody labeled with red fluorescence, the cells fluoresced red. Observation of the non-tandem double-enzyme co-display strain JY-QΔ*RS09985::SOP-his*/p519n-*SOM-flag* under an inverted fluorescence microscope following binding with primary and secondary antibodies (Fig. 5E) confirmed the successful display of PETase and MHETase on the surface of JY-Q, respectively.

FASTPETase, a novel enzyme developed through machine learning algorithms based on the natural PETase. This enzyme exhibits efficient plastic degradation within a temperature range of 28 °C–52 °C, surpassing the depolymerization rate of natural PETase. The FASTPETase was used in construction of the tandem two-enzyme co-display strain. To obtain the sequence information of FASTPETase, the PDB protein database was referenced, and the gene underwent codon optimization before being imported into JY-Q. The single-enzyme display strain, JY-Q/p519n-*signal(oprF)-cOmpa-fastpetase-flag* (abbreviated as JY-Q/p519n-*SOF*), was then constructed. Subsequently, the tandem dual-enzyme co-display strain, JY-Q/p519n-*signal(oprF)-cOmpa-fastpetase-mhetase-his* (abbreviated as JY-Q/p519n-*sfm-6his*), was obtained (Fig. 6A).

Verification of the tandem double-enzyme co-display strain was conducted in three aspects: (1) SDS-PAGE analysis confirmed the heterologous expression of the chimerase FASTPETase-MHETase in JY-Q, with the expected chimerase size at 92.6 KDa, demonstrating successful expression and purification of the target protein (Fig. 6B, lane 4). (2) BHET degradation experiments were performed on both the tandem double-enzyme co-exhibiting strain JY-Q/p519n-*SOFM-his* and the strain JY-Q/p519n-*SOF*. Results revealed that the strain JY-Q/p519n-*SOF* which displaying FASTPETase, can degrade BHET and produce a substantial amount of MHET. In contrast, the tandem two-enzyme co-display strain JY-Q/p519n-*SOFM-his* can completely degrade BHET to TPA (Fig. 6C), indicating catalytic activity of the chimerase displayed on the cell surface, which encompassing both PETase and MHETase activities. (3) Indirect immunofluorescence was employed for cell surface localization verification. JY-Q/p519n-*SOFM-his*, carrying a His-tag, was bound by a mouse anti-His antibody and subsequently treated with a green fluorescent-labeled secondary antibody. Fluorescence microscopy revealed the detection of green fluorescence, confirming the successful display of the FASTPETase-MHETase chimerase on the cell surface (Fig. 6D).

The strains generated through the aforementioned two strategies, namely JY-Q/Δ*RS09985::SOP-his*/p519n-*SOM-flag* and JY-Q/p519n-*SOFM-his*, underwent a PET film degradation test and a PET powder degradation test. In the PET film degradation test the surface erosion of the PET film was detected using scanning electron microscopy, and detectable PET damage was observed for both JY-Q/Δ*RS09985::SOP-his*/p519n-*SOM-flag* and JY-Q/p519n-*SOFM-his* strains. However, control groups including wild-type JY-Q, JY-Q/p519n-*FM-6his*, and JY-Q/p519n-*MF-6his*, displayed no membrane damage. This further confirmed that the PETase and MHETase in the strains JY-QΔ*RS09985::SOP-his*/p519n-*SOM-flag* and JY-Q/p519n-*SOFM-his* had been successfully displayed on the cell surface and exerted a catalytic effect in degrading PET (Fig. 7). The degradation of PET powder by strains JY-QΔ*RS09985::SOP-his*/p519n-*SOM-flag* and JY-Q/p519n-*SOFM-his* was also conducted, and intermediate metabolites were detected (Fig. S3). It can be seen that the degradation efficiency can be further improved.

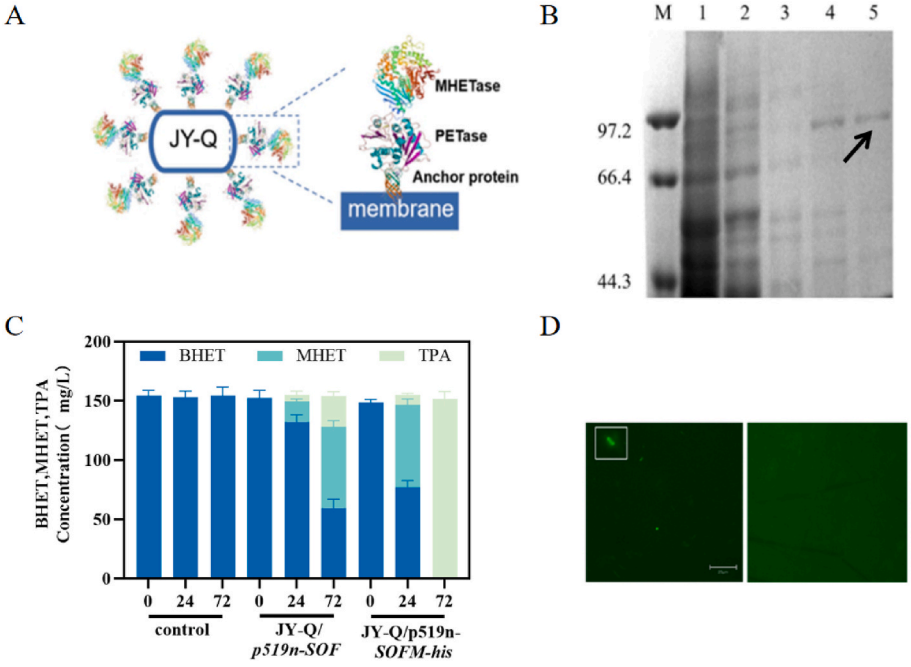

Fig. 6. Determination of the degradation performance of tandem double-enzyme co-display Strain. (A) Schematic representation of tandem double-enzyme co-display; (B) FASTPETase-MHETase Chimerase purified from JY-Q/p519n-*SOFM-his*. Lanes 1–5 are supernatant, effluent, 80 mM imidazole elution, 150 mM imidazole elution, and 200 mM imidazole elution, respectively; (C) BHET degradation by JY-Q/p519n-*SOF* and JY-Q/p519n-*SOFM-his*; (D) Indirect immunofluorescence results for tandem double-enzyme co-display strain and control group.

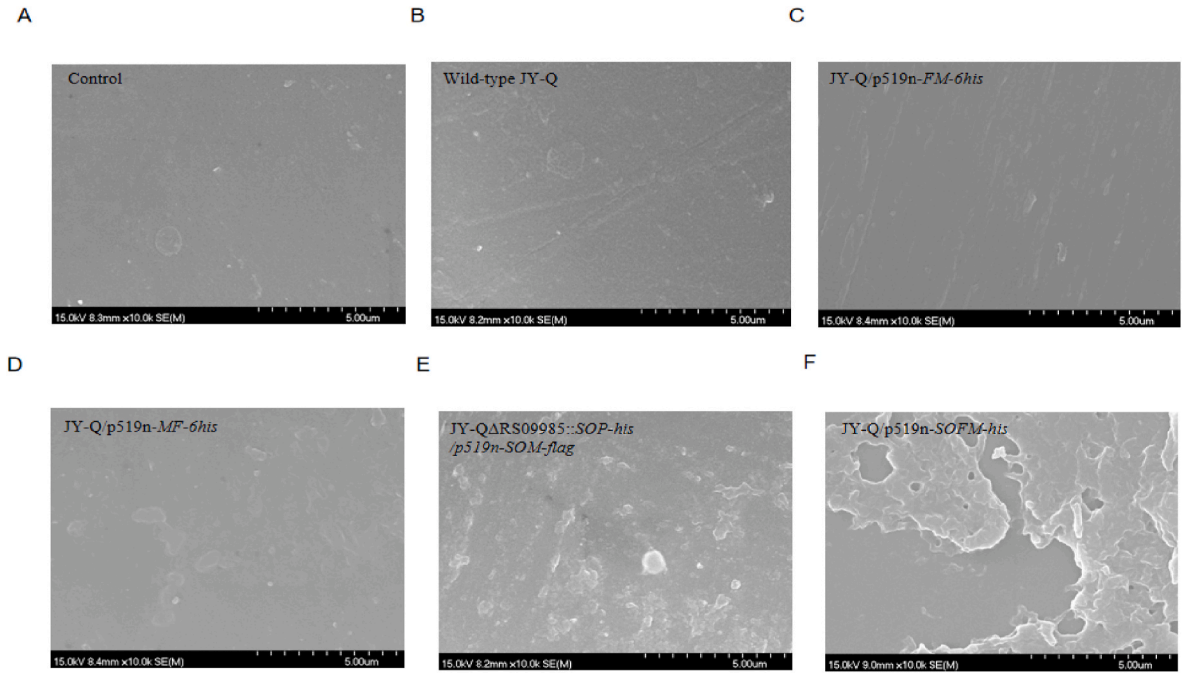

Fig. 7. Processing effect of constructed strains on PET film observed by SEM. (A) Control group; (B) Wild-type JY-Q; (C) JY-Q/p519n-*FM-6his*; (D) JY-Q/p519n-*MF-6his*; (E) JY-QΔRS09985*SOP-his/p519n-SOM-flag*; (F) JY-Q/p519n-*SOFM-his*.

3.6. Degradation of combined pollutants of polyethylene terephthalate and phthalate esters by JY-Q-R1-R4-SFM and JY-Q-R1-R4-SFM-TPH

During the degradation of combined pollution of BHET and DBP, there was no significant change in substrate concentration during the negative control group and wild-type JY-Q group. Strain JY-Q-R1-R4 could transform DBP to produce PA. JY-Q-R1-R4-SFM can degrade both BHET and DBP simultaneously, but complete degradation of BHET and DBP was not achieved, as TPA and PA accumulated. However, with the integration of $tphA2_{II}A3_{II}B_{II}A1_{II}$, JY-Q-R1-R4-SFM-TPH can degrade BHET completely (Fig. 8).

Moreover, JY-Q-R1-R4-SFM showed obvious green fluorescence by indirect immunofluorescence assay (Fig. S4A), and no fluorescence reaction was detected in the control group of chassis strain JY-Q-R1-R4 (Fig. S4B), indicating that *sfm-6his* successfully demonstrated the enzyme to the cell surface after integration into genome of strain JY-Q-R1-R4.

Degradation of DBP by JY-Q-R1-R4-SFM-TPH is efficient (98 % removal in 16 h), while removal of the long-chain PAEs DEHP was 45 %. The results indicated that JY-Q-R1-R4-SFM-TPH could degrade both short and long-chain PAEs. Besides, the control strain JY-Q and negative control group showed no degradation of DBP and DEHP (Fig. 9). After 28 days of incubation, the PET films in each group were removed and the surface erosion of the PET film was detected using scanning electron microscopy, and detectable PET damage was observed for JY-Q-R1-R4-SFM group (Fig. S5A) and JY-Q-R1-R4-SFM-TPH group (Fig. 10C). However, control group, wild-type JY-Q and JY-Q-R1-R4 displayed no membrane damage (Fig. 10A–B and Fig. S5B). Moreover, when cells suspension was supplemented during the incubation period, the surface erosion of the PET film was more distinct (Fig. 10D). These results confirmed that the PETase, MHETase, TPADO, DCDDH and esterase in the strains had been successfully expressed and exerted a catalytic effect

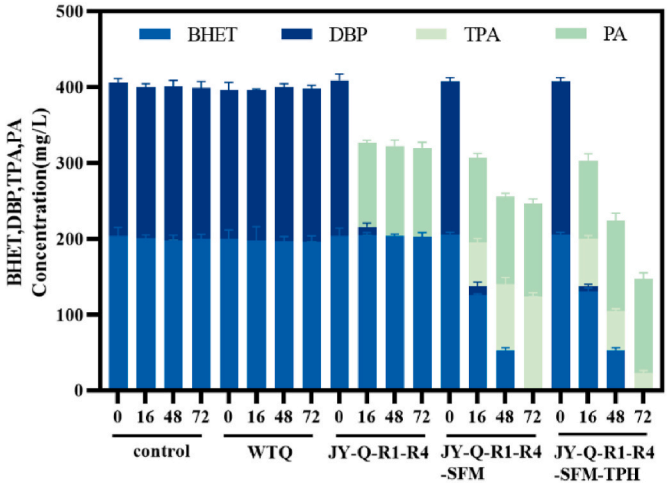

Fig. 8. Degradation of combined pollution of BHET and DBP. Control, control group without adding cell suspension; WTQ, group with cell suspension of wild-type JY-Q; JY-Q-R1-R4, group with cell suspension of JY-Q-R1-R4; JY-Q-R1-R4-SFM, group with cell suspension of JY-Q-R1-R4-SFM; JY-Q-R1-R4-SFM-TPH, group with cell suspension of JY-Q-R1-R4-SFM-TPH.

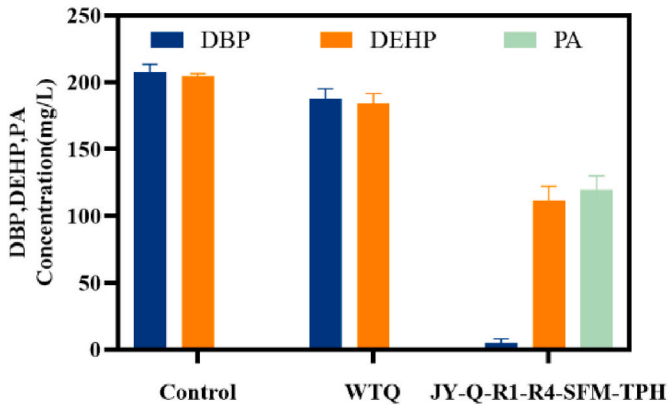

Fig. 9. Degradation of combined pollution of DBP and DEHP. Control, control group without adding cell suspension; WTQ, group with cell suspension of wild-type JY-Q; JY-Q-R1-R4-SFM-TPH, group with cell suspension of JY-Q-R1-R4-SFM-TPH.

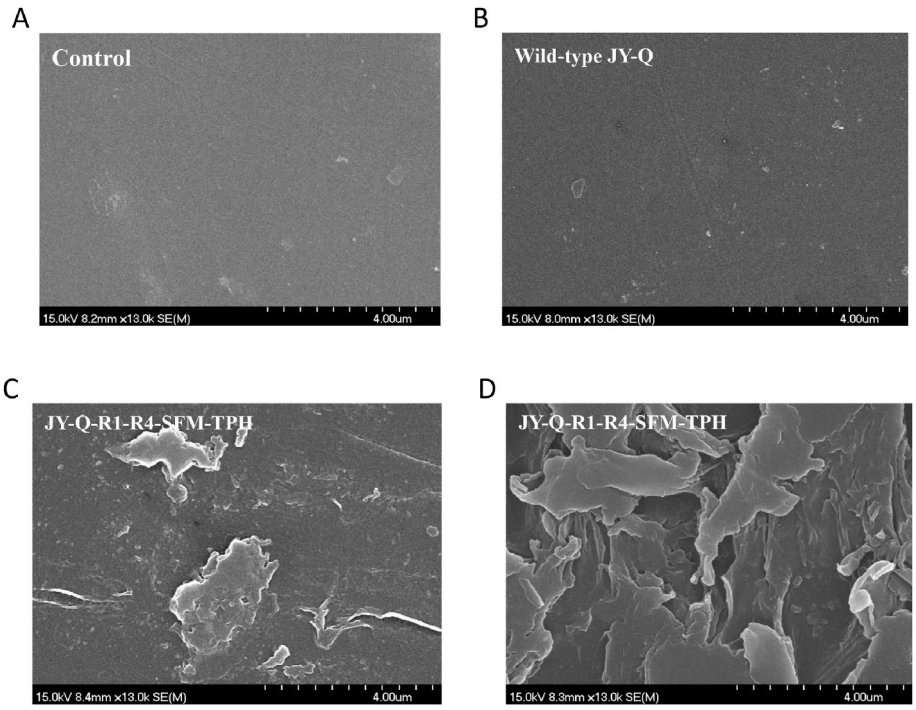

Fig. 10. Processing effect of constructed strains on PET film observed by SEM. (A) Control group; (B) Wild-type JY-Q; (C) JY-Q-R1-R4-SFM-TPH; (D) JY-Q-R1-R4-SFM-TPH with additional cells suspension supplemented during the incubation period.

in degrading combined pollutants of PET and PAEs.

4. Discussion

Enzyme-based PET degradation is an emerging technology and environmentally friendly compared with traditional physical or chemical degradation processes. Given that PET is a highly crystalline polymer, it is difficult for PET to crossing cell membranes. Surface display systems and whole-cell catalysts have become prominent choices for plastic degradation. The co-display of PETase and MHETase on the surface of *Pseudomonas* sp. JY-Q demonstrates the feasibility of PET biodegradation. In this investigation, endogenous anchoring proteins Signal(OprF)-cOmpA and cOmpA, suitable for cell surface display, were identified and engineered in *Pseudomonas* sp. JY-Q. The efficacy of these two anchored proteins for surface display was confirmed through the localization of green fluorescent protein and indirect immunofluorescence experiments. By utilizing the aforementioned anchor proteins, PETase, MHETase, and the chimeric FASTPETase-MHETase were successfully displayed on the surface of JY-Q cells. It was established that the PET hydrolase exhibited catalytic activity, rendering it suitable for PET biodegradation. The efficiency of the dual enzyme's surface display will be further optimized in subsequent studies.

This research not only presents a strategy for biodegrading PET but also showcases the versatility of employing *Pseudomonas* sp. JY-Q as a platform for expressing and surface displaying PET hydrolase. This finding holds relevance in inspiring the development of other high-performance collaborative surface display systems. Furthermore, genomic analysis revealed a downstream pathway for PET degradation in *Pseudomonas* sp. JY-Q, laying the groundwork for subsequent efforts to construct a comprehensive metabolic pathway for PET degradation in JY-Q.

In this study, JY-Q-R1-R4, which has integrated *estR1* and *estR4* esterase genes, was used as the chassis strain. The genes encoding anchor and PET hydrolase fusion protein, as well as genes encoding TPA 1,2-dioxygenase and 1,2-dihydroxy-3,5-cyclohexadiene-1,4- dicarboxylate dehydrogenase, were integrated into the genome to construct a recombinant strain Q-R1-R4-SFM-TPH that can degrade PET and PAEs at the same time. Compared with the *E. coli* and yeast display platforms used in previous studies to display PET hydrolase enzymes, the chassis strains selected in this study were PAEs-degrading strains and were highly stress-resistant and able to adapt to harsh environments. In addition, in the selection of anchor proteins, we screened the endogenous anchor protein OmpA, truncated it and replaced the signal peptide, and constructed an anchoring motif that was more suitable for the chassis strain to construct a reasonable surface display platform.

In general, our research provides new ideas and methods for the biodegradation of combined pollutants of PET and PAEs. Through the precise selection of chassis strains, the ingenious construction of the display system, and the establishment of the dual-enzyme co-display system, it is potential for successfully degradation of combined pollutants of PET and PAEs.

CRediT authorship contribution statement

Haixia Wang: Writing – review & editing, Writing – original draft, Supervision, Investigation, Data curation. **Jiahong Zhu:** Writing – original draft, Visualization, Investigation, Data curation. **Meng Sun:** Writing – original draft, Investigation, Data curation. **Mengjie Gu:** Visualization, Investigation, Data curation. **Xiya Xie:** Writing – original draft, Visualization, Investigation, Data curation. **Tongtong Ying:** Visualization, Investigation, Data curation. **Zeling Zhang:** Methodology, Investigation, Data curation. **Weihong Zhong:** Writing – review & editing, Supervision, Funding acquisition, Conceptualization.

Declaration of competing interest

The authors declare that they have no known competing financial interests or personal relationships that could have appeared to influence the work reported in this paper.

Acknowledgements

This work was financially supported by the National Key Research and Development Program of China (grant number 2021YFA0909500).

Appendix A. Supplementary data

Supplementary data to this article can be found online at https://doi.org/10.1016/j.synbio.2024.08.001.

References

[1] Webb HK, Arnott J, Crawford RJ, Ivanova EP. Plastic degradation and its environmental implications with special reference to poly(ethylene terephthalate). Polymers 2012;5(1):1–18. https://doi.org/10.3390/polym5010001.

[2] Gregory MR. Environmental implications of plastic debris in marine settings—entanglement, ingestion, smothering, hangers-on, hitch-hiking and alien invasions. Philos Trans R Soc Lond B Biol Sci 2009;364(1526):2013–25. https://doi.org/10.1098/rstb.2008.0265.

[3] Kawai F, Kawabata T, Oda M. Current knowledge on enzymatic PET degradation and its possible application to waste stream management and other fields. Appl Microbiol Biotechnol 2019;103(11):4253–68. https://doi.org/10.1007/s00253-019-09717-y.

[4] Yoshida S, Hiraga K, Takehana T, Taniguchi I, Yamaji H, Maeda Y, Toyohara K, Miyamoto K, Kimura Y, Oda K. A bacterium that degrades and assimilates poly (ethylene terephthalate). Science 2016;351(6278):1196–9. https://doi.org/10.1126/science.aad6359.

[5] Hachisuka S, Nishii T, Yoshida S. Development of a targeted gene disruption system in the poly(ethylene terephthalate)-degrading bacterium *Ideonella sakaiensis* and its applications to PETase and MHETase genes. Appl Environ Microbiol 2021;87(18). https://doi.org/10.1128/AEM.00020-21.

[6] Yoshida S, Hiraga K, Taniguchi I, Oda K. *Ideonella sakaiensis*, PETase, and MHETase: from identification of microbial PET degradation to enzyme characterization. Methods Enzymol 2021;648:187–205. https://doi.org/10.1016/bs.mie.2020.12.007.

[7] Taniguchi I, Yoshida S, Hiraga K, Miyamoto K, Kimura Y, Oda K. Biodegradation of PET: current status and application aspects. ACS Catal 2019;9(5):4089–105. https://doi.org/10.1021/acscatal.8b05171.

[8] Kaabel S, Therien J, Deschênes C, Duncan D, Auclair K. Enzymatic depolymerization of highly crystalline polyethylene terephthalate enabled in moist-solid reaction mixtures. Proc Natl Acad Sci U S A 2021;118(29):e2026452118. https://doi.org/10.1073/pnas.2026452118|1of6.

[9] Gao R, Pan HJ, Lian JZ. Recent advances in the discovery, characterization, and engineering of poly (ethylene terephthalate) (PET) hydrolases. Enzym Microb Technol 2021;150. https://doi.org/10.1016/j.enzmictec.2021.109868.

[10] Palm GJ, Reisky L, Böttcher D, Müller H, Michels EAP, Walczak MC, Berndt L, Weiss MS, Bornscheuer UT, Weber G. Structure of the plastic-degrading *Ideonella sakaiensis* MHETase bound to a substrate. Nat Commun 2019;10. https://doi.org/10.1038/s41467-019-09326-3.

[11] Graf LG, Michels E, Yew Y, Liu W, Weber G. Structural analysis of PET-degrading enzymes PETase and MHETase from *Ideonella sakaiensis*. Methods Enzymol 2021;648:337–56. https://doi.org/10.1016/bs.mie.2020.12.015.

[12] Knott BC, Erickson E, Allen MD, Gado JE, Graham R, Kearns FL, Pardo I, Topuzlu E, Anderson JJ, Austin HP, Dominick G, Johnson CW, Rorrer NA, Szostkiewicz CJ, Copié V, Payne CM, Woodcock HL, Donohoe BS, Beckham GT, McGeehan JE. Characterization and engineering of a two-enzyme system for plastics depolymerization. Proc Natl Acad Sci U S A 2020;117(41):25476–85. https://doi.org/10.1073/pnas.2006753117.

[13] Eiamthong B, Meesawat P, Wongsatit T, Jitdee J, Sangsri R, Patchsung M, Aphicho K, Suraritdechachai S, Huguenin-Dezot N, Tang S, Suginta W, Paosawatyanyong B, Babu MM, Chin JW, Pakotiprapha D, Bhanthumnavin W, Uttamapinant C. Discovery and genetic code expansion of a polyethylene terephthalate (pet) hydrolase from the human saliva metagenome for the degradation and bio-functionalization of PET. Angew Chem Int Ed Engl 2022;61(37). https://doi.org/10.1002/anie.202203061.

[14] Buhari SB, Nezhad NG, Normi YM, Shariff FM, Leow TC. Insight on recently discovered PET polyester-degrading enzymes, thermostability and activity analyses. 3 Biotech 2024;14(1). https://doi.org/10.1007/s13205-023-03882-8.

[15] Qiu JR, Chen YX, Zhang LQ, Wu JZ, Zeng XH, Shi XG, Liu LM, Chen JF. A comprehensive review on enzymatic biodegradation of polyethylene terephthalate. Environ Res 2024;240. https://doi.org/10.1016/j.envres.2023.117427.

[16] Shi LX, Zhu LL. Recent advances and challenges in enzymatic depolymerization and recycling of PET wastes. Chembiochem 2023. https://doi.org/10.1002/cbic.202300578.

[17] Yin QD, Zhang JX, Ma S, Gu T, Wang MF, You SP, Ye S, Su RX, Wang YX, Qi W. Efficient polyethylene terephthalate biodegradation by an engineered *Ideonella sakaiensis* PETase with a fixed substrate-binding W156 residue. Green Chem 2023. https://doi.org/10.1039/d3gc03663d.

[18] Liebminger S, Eberl A, Sousa F, Heumann S, Fischer-Colbrie G, Cavaco-Paulo A, Guebitz GM. Hydrolysis of PET and bis-(benzoyloxyethyl) terephthalate with a new polyesterase from *Penicillium citrinum*. Biocatal Biotransform 2007;25(2–4):171–7. https://doi.org/10.1080/10242420701379734.

[19] Freudl, Roland. Insertion of peptides into cell-surface-exposed areas of the *Escherichia coli* OmpA protein does not interfere with export and membrane assembly. Gene 1989;82(2):229–36. https://doi.org/10.1016/0378-1119(89)90048-6.

[20] Gallus S, Peschke T, Paulsen M, Burgahn T, Niemeyer CM, Rabe KS. Surface display of complex enzymes by *in situ* SpyCatcher-SpyTag interaction. Chembiochem 2020;21(15):2126–31. https://doi.org/10.1002/cbic.202000102.

[21] Hui CY, Guo Y, Liu L, Zheng HQ, Wu HM, Zhang LZ, Zhang W. Development of a novel bacterial surface display system using truncated OmpT as an anchoring motif. Biotechnol Lett 2019;41(6–7):763–77. https://doi.org/10.1007/s10529-019-02676-4.

[22] Dvorák P, Bayer EA, de Lorenzo V. Surface display of designer protein scaffolds on genome-reduced strains of *Pseudomonas putida*. ACS Synth Biol 2020;9(10):2749–64. https://doi.org/10.1021/acssynbio.0c00276.

[23] Lee SH, Choi JI, Han MJ, Choi JH, Lee SY. Display of lipase on the cell surface of *Escherichia coli* using OprF as an anchor and its application to enantioselective resolution in organic solvent. Biotechnol Bioeng 2010;90(2):223–30. https://doi.org/10.1002/bit.20399.

[24] Lee SH, Lee SY. Cell surface display of poly(3-hydroxybutyrate) depolymerase and its application. J Microbiol Biotechnol 2020;30(2):244–7. https://doi.org/10.4014/jmb.2001.01042.

[25] Confer AW, Ayalew S. The OmpA family of proteins: roles in bacterial pathogenesis and immunity. Vet Microbiol 2013;163(3–4):207–22. https://doi.org/10.1016/j.vetmic.2012.08.019.

[26] Hu JY, Chen YJ. Constructing *Escherichia coli* co-display systems for biodegradation of polyethylene terephthalate. Bioresour Bioprocess 2023;10(1). https://doi.org/10.1186/s40643-023-00711-x.

[27] Han L, Liang B, Song JX. Rational design of engineered microbial cell surface multi-enzyme co-display system for sustainable NADH regeneration from low-cost biomass. J Ind Microbiol Biotechnol 2018;45(2):111–21. https://doi.org/10.1007/s10295-018-2002-z.

[28] Ishii J, Okazaki F, Djohan AC, Hara KY, Asai-Nakashima N, Teramura H, Andriani A, Tominaga M, Wakai S, Kahar P, Yopi, Prasetya B, Ogino C, Kondo A. From mannan to bioethanol: cell surface co-display of β-mannanase and β-mannosidase on yeast *Saccharomyces cerevisiae*. Biotechnol Biofuels 2016;9. https://doi.org/10.1186/s13068-016-0600-4.

[29] Sun YF, Lin Y, Zhang JH, Zheng SP, Ye YR, Liang XX, Han SY. Double *Candida antarctica* lipase B co-display on *Pichia pastoris* cell surface based on a self-processing foot-and-mouth disease virus 2A peptide. Appl Microbiol Biotechnol 2012;96(6):1539–50. https://doi.org/10.1007/s00253-012-4264-0.

[30] Gercke D, Furtmann C, Tozakidis I, Jose J. Highly crystalline post-consumer PET waste hydrolysis by surface displayed PETase using a bacterial whole-cell biocatalyst. ChemCatChem 2021;13(15):3479–89. https://doi.org/10.1002/cctc.202100443.

[31] Heyde SAH, Bååth JA, Westh P, Norholm MHH, Jensen K. Surface display as a functional screening platform for detecting enzymes active on PET. Microb Cell Factories 2021;20(1). https://doi.org/10.1186/s12934-021-01582-7.

[32] da Costa AM, de Oliveira Lopes VR, Vidal L, Nicaud J-M, de Castro AM, Coelho MAZ. Poly(ethylene terephthalate) (PET) degradation by *Yarrowia lipolytica*: investigations on cell growth, enzyme production and monomers consumption. Process Biochem 2020;95:81–90. https://doi.org/10.1016/j.procbio.2020.04.001.

[33] Chen Z, Xiao Y, Weber G, Wei R, Wang Z. Yeast cell surface display of bacterial PET hydrolase as a sustainable biocatalyst for the degradation of polyethylene terephthalate. Methods Enzymol 2021;5(648):457–77. https://doi.org/10.1016/bs.mie.2020.12.030.

[34] Loll-Krippleber R, Sajtovich VA, Ferguson MW, Ho BD, Burns AR, Payliss BJ, Bellissimo J, Peters S, Roy PJ, Wyatt HDM, Brown GW. Development of a yeast whole-cell biocatalyst for MHET conversion into terephthalic acid and ethylene glycol. Microb Cell Factories 2022;21(1). https://doi.org/10.1186/s12934-022-02007-9.

[35] Zhang ZL, Mei XT, He ZL, Xie XY, Yang Y, Mei CY, Xue D, Hu T, Shu M, Zhong WH. Nicotine metabolism pathway in bacteria: mechanism, modification, and application. Appl Microbiol Biotechnol 2022;106(3):889–904. https://doi.org/10.1007/s00253-022-11763-y.

[36] Huang C, Shan L, Chen Z, He Z, Li J, Yang Y, Shu M, Pan F, Jiao Y, Zhang F, Linhardt RJ, Zhong W. Differential effects of homologous transcriptional regulators NicR2A, NicR2B1, and NicR2B2 and endogenous ectopic strong promoters on nicotine metabolism in *Pseudomonas* sp. strain JY-Q. Appl Environ Microbiol 2021;87(3):e02457. https://doi.org/10.1128/AEM.02457-20. 20.

[37] Chakraborty P, Bharat GK, Gaonkar O, Mukhopadhyay M, Chandra S, Steindal EH, Nizzetto L. Endocrine-disrupting chemicals used as common plastic additives: levels, profiles, and human dietary exposure from the Indian food basket. Sci Total Environ 2022;810:152200. https://doi.org/10.1016/j.scitotenv.2021.152200.

[38] Wang X, Wu H, Wang X, Wang H, Zhao K, Ma B, Lu Z. Network-directed isolation of the cooperator *Pseudomonas aeruginosa* ZM03 enhanced the dibutyl phthalate degradation capacity of *Arthrobacter nicotianae* ZM05 under pH stress. J Hazard Mater 2021;410:124667. https://doi.org/10.1016/j.jhazmat.2020.124667.

[39] Schmidt N, Castro-Jiménez J, Fauvelle V, Ourgaud M, Sempéré R. Occurrence of organic plastic additives in surface waters of the Rhone River (France). Environ Pollut 2020;257. https://doi.org/10.1016/j.envpol.2019.113637.

[40] Hou Z, Pan H, Gu M, Chen X, Ying T, Qiao P, Cao J, Wang H, Hu T, Zheng L, Zhong W. Simultaneously degradation of various phthalate esters by *Rhodococcus* sp. AH-ZY2: strain, omics and enzymatic study. J Hazard Mater 2024;474:134776. https://doi.org/10.1016/j.jhazmat.2024.134776.

[41] Zhang Z. Construction of PETase surface-displaying cells from *Pseudomonas* sp. JY-Q; 2022.

[42] Jumper J, Evans R, Pritzel A, Green T, Hassabis D. Highly accurate protein structure prediction with AlphaFold. Nature 2021;596(7873):583–9. https://doi.org/10.1038/s41586-021-03819-2.

[43] Sasoh M, Masai E, Ishibashi S, Hara H, Kamimura N, Miyauchi K, Fukuda M. Characterization of the terephthalate degradation genes of *Comamonas* sp. Strain E6. Appl Environ Microbiol 2006;72(3):1825–32. https://doi.org/10.1128/AEM.72.3.1825-1832.2006.

[44] Wang X, Bernstein HD. The *Escherichia coli* outer membrane protein OmpA acquires secondary structure prior to its integration into the membrane. J Biol Chem 2022; 298(4). https://doi.org/10.1016/j.jbc.2022.101802.

[45] Smith SGJ, Mahon V, Lambert MA, Fagan RP. A molecular swiss army knife: OmpA structure, function and expression. FEMS Microbiol Lett 2007;273(1):1–11. https://doi.org/10.1111/j.1574-6968.2007.00778.x.

[46] Song BF, Yang XJ, Sun HN, Yu LQ, Ma JZ, Wu ZJ, Cui YD. Immunogenicity of amino acids 1-150 of *Streptococcus* GapC displayed on the surface of *Escherichia coli*. Microb Pathog 2017;105:288–97. https://doi.org/10.1016/j.micpath.2017.02.003.